In: Advances in Communications … Volume 11
Editor: Anthony V. Stavros
ISBN: 978-1-63483-283-0

Chapter 6

DETECTION OF SPATIALLY DISTRIBUTED SIGNALS BY GENERALIZED RECEIVER USING RADAR SENSOR ARRAYS IN WIRELESS COMMUNICATIONS

Vyacheslav Tuzlukov'
School of Electronics Engineering, College of IT Engineering,
Kyungpook National University, Daegu, South Korea

ABSTRACT

We consider a problem of detecting a random spatially distributed signal source by an array of sensors based on the generalized approach to signal processing (GASP) in noise. We derive some generalized receiver (GR) structures under several assumptions on the available statistics. The GR performance is evaluated and the effect of source angular spread is investigated. We notice the degrees of freedom of detection statistics distributions depend on both the signal angular spread and the number of data snapshots. At the high signal-to-noise ratio and with small degrees of freedom, increasing in angular spread improves the detection performance. With large degrees of freedom the increasing in angular spread reduces the detection performance. A comparison between GR and conventional beamformer is carried out by computer simulations. The results indicate a superiority of GR implementation as the angular spread becomes large over the conventional beamformer detector.

1. INTRODUCTION

In the majority of cases, a large class of modem array processing techniques has been designed for point sources, i.e., spatially discrete sources of electromagnetic energy. In many applications, the transmitter is best modelled as a distributed, rather than a point source. The distributed sources appear to have certain angular spread with a mean direction of an'ival

* Email: tuzlukov@ee.knu.ac.kr , Website: http://spl.knu.ac.kr

(DOA) The point source model is only an approximation of the practical situation when there is a large distance between the source and the receiver array.

The principal mechanism to make the source appear to be distributed in a space is diffuse (irresolvable) and specular (resolvable) multipath caused by scattering of the propagation waves. For example, experimental results obtained in urban wireless communications reported significant angular scattering distributions due to local scattering and reflection from mobile stations [1]–[3] and base stations [4], [5]. The characterization of the power azimuth spectrum shows that angular spreads as large as 25° have been observed. The amount of angular spread is highly dependent on the scattering around the mobile, the height of the base station, and the distance between the base station and the mobile station. Secondary, but equally important, mechanism is transmitter motion. If the source moves significantly during the observation interval or coherent integration time, it will appear to be distributed rather that discrete.

The angular spread has a significant impact on any array processing algorithms [6], i.e., the signal-to-noise ratio (*SNR*) gain of the array is reduced as the angular spread is increased [7], causing possible performance degradation. In passive array signal processing area, the problems under study concern the extraction of information from measurements using an array of radar sensors. Given the observations of the radar sensor outputs, the objective is to estimate the unknown parameters associated with the waveforms or target return signals corrupted by the noise.

We start with a simple and computationally efficient detection scheme. If the "noise only" hypothesis is rejected, other algorithms are used to estimate the number of the spatially distributed sources and their unknown parameters, such as radar range and bearing. Prior work on distributed sources focuses primarily on source localization and DOA estimation [8]–[11]. Estimation of the number of spatially distributed sources has also been studied in [8].

Subspace detectors have been studied in [12], [13] for the cases where the spatially distributed signal lies in a deterministic subspace. The case of detecting the Gaussian signals with a low-rank covariance matrix and matched subspace detectors have been developed based on the generalized likelihood ratio test (GLRT). In both cases, the subspace in which the signals lie is assumed to be known. In other words, the dimension and rank of the signal subspace are assumed to be known a priori. This assumption does not hold in practical situations. The rank, orientation, and strength of the signal subspace vary along with the signal angular spread, DOA, and the energy distribution function. In this case, the unknown parameters may be estimated based on the maximum likelihood principle.

In the present paper, we develop the generalized receiver (GR) constructed based on the generalized approach to signal processing (GASP) in noise [14]–[19] for spatially distributed signal sources and study the GR performance depending on the angular spread. The idea to employ the generalized receiver (GR) for the radar sensor array has been triggered by the purpose to improve the detection performance of radar sensor systems at the low *SNR*. The GR can be described as a combination of the optimal detector in the Neyman-Pearson (NP) criterion sense and energy detector (ED) [14]–[16]. The main function of GR ED is to detect a signal and the main function of the GR NP is to confirm a detection of the searched signal and to define the detected signal parameters as discussed in detail in [16, Chapter 7, pp. 685–692].

A great difference between the GR ED and conventional ED is a presence of additional linear system, for example, the bandpass filter, at the GR input. This bandpass filter can be considered as the source of additional (reference) noise which does not contain the target return signal from spatially distributed signal source. The GR allows us to formulate a decision statistics about the target return signal presence or absence based on definition of the jointly sufficient statistics of the mean and variance of the likelihood function [16, Chapter 3] while the optimal detectors of classical and modern detection theories make a decision about the target return signal presence or absence based on definition of the mean of the likelihood function, only, and the conventional ED employed by radar sensor array system defines a decision statistics with respect to the target return signal presence or absence based on determination of the variance of the likelihood function only.

Thus, an implementation of GR in radar sensor array systems allows us to extract more information from the likelihood function and make a more accurate decision about the target return signal presence or absence in comparison, for example, with the matched filter (MF) or ED.

Theoretically, the GR can be applied to detect any target return signal, i.e., the signal with known or unknown, deterministic or random parameters. The GR implementation in radar and wireless communication is discussed in [19] and [20]–[25] and [19], respectively. The signal detection performance improvement using GR in radar sensor system is investigated in [26]–[31]. The first attempt to investigate the GR employment in cognitive radio (CR) systems has been discussed in [32].

In the present chapter, we first look at the case of known parameters. In this case, the GR can be approximated as a subspace beamformer. The detection performance depends on the detection statistic distribution and the radar sensor *SNR* at the GR output. The degrees of freedom (DOF) of the detection statistics are determined by the angular spread and the number of data snapshots. If we fix the number of data snapshots, we show that increasing in angular spread reduces the mean of the detection statistics that degrades the detection performance, and at the same time reduces its variance improving the detection performance.

Within a certain range of DOF, the detection performance is improved with increasing in the angular spread, up to a point, and then is degraded slowly. We consider the case when the various parameters, such as the signal direction, angular spread, power, and noise power are unknown. We derive the GLRT GR and evaluate its performance by computer simulation. We demonstrate that the GLRT GR has a significant performance advantage compared with conventional beamformers of modern detection theory as the angular spread becomes large.

The reminder of this chapter is organized as follows. Section 2 presents a brief description of the general GR flowchart and the main functioning principles and decision statistics obtained at the GR output. The main statements of signal model, the brief description of signal subspace, and detection problem are delivered in Section 3. Several types of the GR beamformers with various set of unknown parameters are discussed in Section 4. Section 5 introduces the performance analysis when the parameters are known. Numerical results obtained under simulation are presented and discussed in Section 6. Finally, the conclusion remarks are made in Section 7.

2. CONVENTIONAL GR

As we mentioned before, the GR is constructed in accordance with GASP in noise [14]–[16]. The GASP introduces an additional noise source that does not carry any information about the incoming target return signal with the purpose to improve the signal processing system performance. This additional noise can be considered as the reference noise without any information about the signal to be detected. The jointly sufficient statistics of the mean and variance of the likelihood function is obtained under GASP employment, while the classical and modern signal processing theories can deliver only a sufficient statistics of the mean or variance of the likelihood function. Thus, GASP implementation allows us to obtain more information about the target return signal incoming at the GR input. Owing to this fact, the detectors constructed on the GASP technology are able to improve the signal detection performance in comparison with other conventional detectors.

The GR consists of three channels (see Figure 1): the GR correlation detector channel (GR CD) – the preliminary filter (PF), the multipliers 1 and 2, the model signal generator (MSG); the GR energy detector (GR ED) channel – the PF, the additional filter (AF), the multipliers 3 and 4, the summator 1; and the GR compensation channel (GR CC) – the summators 2 and 3, the accumulator 1. The threshold apparatus (THRA) device defines the GR threshold.

As we can see from Figure 1, there are two band-pass filters, i.e., the linear systems, at the GR input, namely, the PF and AF. We assume for simplicity that these two filters or linear systems have the same amplitude-frequency characteristics or impulse responses. The AF central frequency is detuned relative to the PF central frequency. There is a need to note the PF bandwidth is matched with the bandwidth of the radio channel or target return signal band-width.

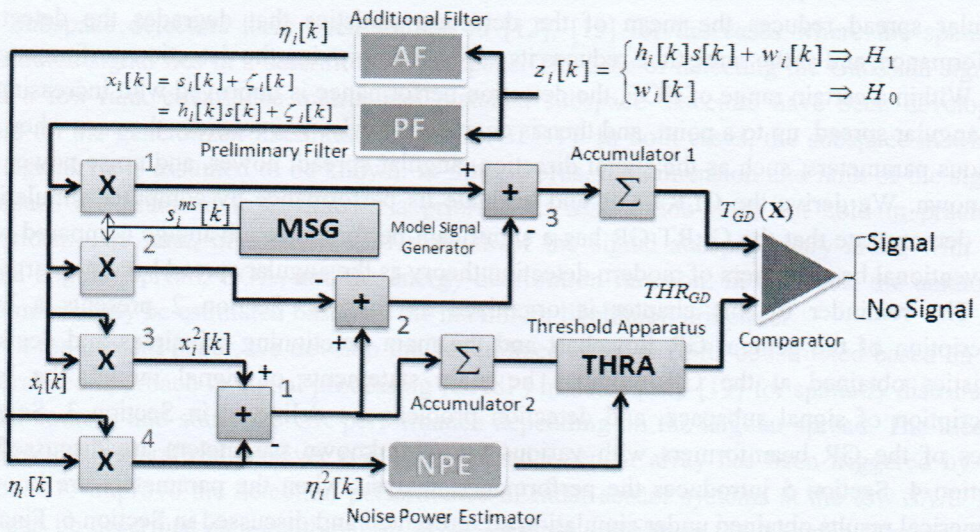

Figure 1. GD structure.

If the detuning value between the PF and AF central frequencies is more than 4 or 5 times the target return signal bandwidth to be detected, i.e., $4 \sim 5\,\Delta f_s$, where Δf_s is the target return

signal bandwidth, we can believe that the processes at the PF and AF outputs are uncorrelated because the coefficient of correlation between them is negligible (not more than 0.05). This fact was confirmed experimentally in [33] and [34]. Thus, the target return signal plus noise can be appeared at the GR PF output and the noise only is appeared at the GR AF output.

The stochastic processes at the AF and PF outputs present the input stochastic samples from two independent frequency-time regions. If the discrete-time noise $w_i[k]$ at the PF and AF inputs is Gaussian, the discrete-time noise $\xi_i[k]$ at the PF output is Gaussian and the reference discrete-time noise $\eta_i[k]$ at the AF output is Gaussian, too, owing to the fact that the PF and AF are the linear systems and we believe that these linear systems do not change the statistical parameters of the input process. Thus, the AF can be considered as a generator of the reference noise with a priori information a "no" target return signal (the reference noise sample) [17, Chapter 5]. The noise at the PF and AF outputs can be presented in the following form:

$$\begin{cases} \xi_i[k] = \sum\limits_{m=-\infty}^{\infty} g_{PF}[m] w_i[k-m] \ ; \\ \eta_i[k] = \sum\limits_{m=-\infty}^{\infty} g_{AF}[m] w_i[k-m] \ , \end{cases} \tag{1}$$

where $g_{PF}[m]$ and $g_{AF}[m]$ are the impulse responses of the PF and AF, respectively.

In a general, under practical implementation of any detector in radar system with sensor array, the bandwidth of the spectrum to be sensed is defined. Thus, the AF bandwidth and central frequency can be assigned, too (the AF bandwidth can not be used by the target return signal because it is out of its spectrum). The case when there are interfering signals within the AF bandwidth, the action of this interference on the GR detection performance, and the case of nonideal condition when the noise at the PF and AF outputs is not the same by statistical parameters are discussed in [28].

Under the hypothesis $\mathcal{H}_1$ ("a yes" target return signal), the GR CD generates the signal component $s_i^{ms}[k]s_i[k]$ caused by interaction between the model signal $s_i^{ms}[k]$, the MSG output, and the incoming target return signal $s_i[k]$, and the noise component $s_i^{ms}[k]\xi_i[k]$ caused by interaction between the model signal $s_i^{ms}[k]$ and the noise $\xi_i[k]$ at the PF output. GR ED generates the signal energy $s_i^2[k]$ and the random component $s_i[k]\xi_i[k]$ caused by interaction between the target return signal $s_i[k]$ and the noise $\xi_i[k]$ at the PF output. The main purpose of the GR CC is to cancel completely in the statistical sense the GR CD noise component $s_i^{ms}[k]\times\ \xi_i[k]$ and the GR ED random component $s_i[k]\xi_i[k]$ based on the same nature of the noise $\xi_i[k]$. The relation between the target return signal to be detected $s_i[k]$ and the model signal $s_i^{ms}[k]$ is defined as:

$$s_i^{ms}[k] = \mu s_i[k] \ , \tag{2}$$

where μ is the coefficient of proportionality.

The main functioning condition under the GR employment in any signal processing system including the radar sensor one is the equality between parameters of the model signal $s_i^{ms}[k]$ and the incoming target return signal $s_i[k]$, for example, by amplitude. Under this condition it is possible to cancel completely in the statistical sense the noise component $s_i^{ms}[k]\times\ \xi_i[k]$ of the GR CD and the random component $s_i[k]\xi_i[k]$ of the GR ED. Satisfying the GR main functioning condition given by (2), $s_i^{ms}[k]=s_i[k]$, $\mu=1$, we are able to detect the target return signal with the high probability of detection at the low *SNR* and define the target return signal parameters with high accuracy. Practical realizations of this condition require increasing in the complexity of GR structure and, consequently, lead us to increasing in computation cost. For example, there is a need to employ the amplitude tracking system or to use the off-line data samples processing. Under the hypothesis $\mathcal{H}_0$ ("a no" target return signal), satisfying the main GR functioning condition $s_i^{ms}[k]=s_i[k]$ we obtain only the background noise $\eta_i^2[k]\ -\xi_i^2[k]$ at the GR output.

Under practical implementation, the real structure of GR depends on specificity of signal processing systems and their applications, for example, the radar sensors systems, adaptive communications systems, cognitive radio systems, satellite communication systems, mobile communication systems and so on. In the present paper, the GR circuitry (Figure 1) is demonstrated with the purpose to explain the main operational principles. Because of this, the GR flowchart presented in Figure 1 should be considered under this viewpoint. Satisfying the ma-in functioning condition $s_i^m[k]=s_i[k]$ for GR, the ideal case, for radar sensor applications, we are able to detect the target return signal with high probability of detection and define accurately its parameters.

In the present chapter, we discuss the GR implementation in radar sensor array systems. Since the presented GR test statistics is defined by the signal energy and noise power, see Eqs. (5) and (7), the equality between the model signal $s_i^m[k]$ and the target return signal to be detected $s_i[k]$, in particular by amplitude, is required that leads us to high circuitry complexity in practice. For example, there is a need to implement the amplitude tracking system or off-line data sample processing. Detailed discussion about the main GR functioning principles if there is no a priori information about the target return signal and there is uncertainty with respect to the target return signal parameters, i.e., the target return signal parameters are random, can be found in [14] and [16, Chapter 6, pp.611–621 and Chapter 7, pp. 631–695].

The complete matching between the model signal $s_i^{ms}[k]$ and the incoming target return signal $s_i[k]$, for example, by amplitude is a very hard problem in practice because the incoming target return signal $s_i[k]$ depends on both the fading and the transmitted signal and it is impractical to estimate the fading gain at the low *SNR*. This matching is possible in the ideal case only. The GD detection performance will be deteriorated under mismatching in parameters between the model signal $s_i^{ms}[k]$ and the incoming target return signal $s_i[k]$ and the impact of this problem is discussed in [35], where a complete analysis about the violation of the main GR functioning requirements is presented. The GR decision statistics requires an estimation of the noise variance σ_η^2 using the reference noise $\eta_i[k]$ at the AF output.

Under the hypothesis $\mathcal{H}_1$, the signal at the PF output, see Figure 1, can be defined as

$$x_i[k] = s_i[k] + \xi_i[k] \,, \tag{3}$$

where $\xi_i[k]$ is the noise at the PF output and

$$s_i[k] = h_i[k]s[k], \tag{4}$$

where $h_i[k]$ are the channel coefficients. Under the hypothesis $\mathcal{H}_0$ and for all i and k, the process $x_i[k] = \xi_i[k]$ at the PF output is subjected to the complex Gaussian distribution and can be considered as the independent and identically distributed (i.i.d.) process.

In ideal case, we can think that the signal at the AF output is the reference noise $\eta_i[k]$ with the same statistical parameters as the noise $\xi_i[k]$. In practice, there is a difference between the statistical parameters of the noise $\eta_i[k]$ and $\xi_i[k]$. How this difference impacts on the GR detection performance is discussed in detail in [16, Chapter 7, pp. 631-695].

The decision statistics at the GR output presented in [14] and [16, Chapter 3] is extended for the case of antenna array when an adoption of multiple antennas and antenna arrays is effective to mitigate the negative attenuation and fading effects. The GR decision statistics can be presented in the following form:

$$T_{GR}(\mathbf{X}) = \sum_{k=0}^{N-1}\sum_{i=1}^{M} 2x_i[k]s_i^{ms}[k] - \sum_{k=0}^{N-1}\sum_{i=1}^{M} x_i^2[k] + \sum_{k=0}^{N-1}\sum_{i=1}^{M} \eta_i^2[k] \underset{\mathcal{H}_0}{\overset{\mathcal{H}_1}{\gtrless}} THR_{GR} \,, \tag{5}$$

where

$$\mathbf{X} = \left[\mathbf{x}(0),\ldots,\mathbf{x}(N-1)\right] \tag{6}$$

is the vector of the random process at the PF output and THR_{GR} is the GR detection threshold.

Under the hypotheses $\mathcal{H}_1$ and $\mathcal{H}_0$ and when the amplitude of the incoming target return signal is equal to the amplitude of the model signal, $s_i^{ms}[k] = s_i[k]$ the GR decision statistics $T_{GD}(\mathbf{X})$ takes the following form, respectively:

$$\begin{cases} \mathcal{H}_1 : T_{GD}(\mathbf{X}) = \sum_{k=0}^{N-1}\sum_{i=1}^{M} s_i^2[k] + \sum_{k=0}^{N-1}\sum_{i=1}^{M} \eta_i^2[k] - \sum_{k=0}^{N-1}\sum_{i=1}^{M} \zeta_i^2[k] \,, \\ \mathcal{H}_0 : T_{GD}(\mathbf{X}) = \sum_{k=0}^{N-1}\sum_{i=1}^{M} \eta_i^2[k] - \sum_{k=0}^{N-1}\sum_{i=1}^{M} \zeta_i^2[k] \,. \end{cases} \tag{7}$$

In (7) the term $\sum_{k=0}^{N-1}\sum_{i=1}^{M} s_i^2[k] = E_s$ corresponds to the average target return signal energy, and the term $\sum_{k=0}^{N-1}\sum_{i=1}^{M} \eta_i^2[k] - \sum_{k=0}^{N-1}\sum_{i=1}^{M} \xi_i^2[k]$ is the background noise at the GR

output. The GR output background noise is a difference between the noise power at the PF and AF outputs. Practical implementation of the GR decision statistics requires an estimation of the noise variance σ_{η}^2 using the reference noise $\eta_i[k]$ at the AF output.

3. PROBLEM STATEMENT

3.1. Signal Model

Assume that we have an array with P sensors with an array response vector $\mathbf{a}(\phi)$, where ϕ denotes the azimuth. The array and all the sources are in the same plane. We assume a narrowband model for all signals and all the signals are defined within the limits of baseband. The signal received by the radar sensor array from a single source is modelled as

$$\mathbf{X}_k = \mathbf{S}_k + \boldsymbol{\xi}_k \ , \ k = 1, \ldots, N \tag{8}$$

where N is the sample size and $\mathbf{X}_k = [x_{k_1}, \ldots, x_{k_P}]$ is the array output at sample reading k; $\mathbf{S}_k$ is the signal received at the radar sensor array elements assumed to be complex Gaussian with zero mean and covariance $E_S \mathbf{R}_S$, where E_S is the total signal energy and $\mathbf{R}_S$ is defined below in (10); $\boldsymbol{\xi}_k$ is the complex Gaussian noise with zero mean and covariance $\mathbf{R}_{\xi}$. The signal and noise are uncorrelated from sample to sample.

The correlation matrix of observation vector $\mathbf{X}_k$ is given by

$$\mathbf{R}_1 = E\{\mathbf{X}_k, \mathbf{X}_k^H\} = E_S \mathbf{R}_S(\phi, \beta) + \mathbf{R}_{\xi}, \tag{9}$$

where $(\cdots)^H$ denotes the complex conjugate transpose and the signal covariance matrix is given by

$$\mathbf{R}_S(\phi, \beta) = \int_{-\pi}^{\pi} E(\theta; \phi, \beta) \mathbf{a}(\theta) \mathbf{a}^H(\theta) d\theta, \tag{10}$$

where ϕ is the source azimuth angle and β is the source angular spread with $0 \le \beta \le 2\pi$; $\mathbf{a}(\theta)$ is the array manifold at the angle θ ; $\mathbf{R}_S(\phi, \beta)$ is the normalized so that

$$Tr[\mathbf{R}_S(\phi, \beta)] = P; \tag{11}$$

$Tr[\cdots]$ denotes the trace of a matrix, $E(\theta; \phi, \beta)$ is the spatial energy distribution of source at the azimuth ϕ. More specifically, we may assume that

$$E(\theta; \phi, \beta) = E(\theta - \phi, \beta) \tag{12}$$

with

$$\int_{-\pi}^{\pi} E(\theta;\phi,\beta)d\theta = 1 . \tag{13}$$

The shape of the energy distribution function depends on the angular spread parameter β. If $\beta = 0^\circ$, $E(\theta;\phi,\beta)$ is the unit pulse. As β is increased, the energy distribution function becomes wider. For simplicity, we consider the uniformly distributed source model, i.e.

$$E(\theta;\phi,\beta) = \begin{cases} \dfrac{1}{\beta}, & \theta \in [\phi - 0.5\beta, \phi + 0.5\beta] \\ 0, & \text{otherwise} . \end{cases} \tag{14}$$

One can also consider a Gaussian type distribution such that

$$E(\theta;\phi,\beta) = \begin{cases} \dfrac{1}{\sqrt{2\pi\beta^2}} \exp\left\{ -\dfrac{(\theta-\varphi)^2}{2\beta^2} \right\}, & \theta \in [\phi - 0.5\beta, \phi + 0.5\beta] \\ 0, & \text{otherwise} . \end{cases} \tag{15}$$

3.2. Signal Subspace

By performing an eigen-decomposition of the matrix $\mathbf{R}_S(\phi,\beta)$, we get

$$\mathbf{R}_S(\phi,\beta) = \mathbf{V}\,\mathbf{\Lambda}\,\mathbf{V}^H = (\mathbf{V}_r\ \mathbf{V}_n) \begin{pmatrix} \mathbf{\Lambda}_r & 0 \\ 0 & \mathbf{\Lambda}_n \end{pmatrix} \begin{pmatrix} \mathbf{V}_r^H \\ \mathbf{V}_n^H \end{pmatrix}, \tag{16}$$

where

$$\begin{cases} \mathbf{V} = (\mathbf{V}_r\ \mathbf{V}_n), \\ \mathbf{\Lambda} = diag(\mathbf{\Lambda}_r, \mathbf{\Lambda}_n), \\ \mathbf{\Lambda}_r = diag(\lambda_1, \ldots, \lambda_r). \end{cases} \tag{17}$$

Here $\mathbf{\Lambda}_r$ consists of the $1 \le r \le P$ largest eigenvalues of $\mathbf{R}_S(\phi,\beta)$ in descending order and $\mathbf{V}_r = (\mathbf{v}_1, \ldots, \mathbf{v}_r)$ contains the corresponding orthonormal eigenvectors. If $\mathbf{R}_S(\phi,\beta)$ is the low-rank matrix with rank r, then

$$\mathbf{R}_S(\phi,\beta) = \mathbf{V}_r\,\mathbf{\Lambda}_r\,\mathbf{V}_r^H . \tag{18}$$

More generally, we will assume that $\mathbf{R}_S(\phi,\beta)$ can be approximated by a rank r matrix. The number of dominant eigenvalues may be defined as the minimum number of eigenvalues whose sum exceeded τP, where $0 \le \tau \le 1$ is close to unity, for example, $\tau = 0.95$. Thus,

$$\mathbf{R}_S(\phi,\beta) \approx \mathbf{V}_r \, \mathbf{\Lambda}_r \, \mathbf{V}_r^H \ . \tag{19}$$

The range space of $\mathbf{V}_r$ is called the signal subspace and its orthogonal complement, called the noise subspace, is spanned by $\mathbf{V}_\xi$. The effective rank of subspace is the number of dominant eigenvalues. The case $\beta = 0^\circ$ corresponds to the point source where the rank $r = 1$, and the signal covariance becomes

$$\mathbf{R}_S(\phi,0) = \mathbf{a}(\phi)\mathbf{a}^H(\phi) . \tag{20}$$

3.3. Detection Problem

The detection problem of a random Gaussian signal in the presence of noise and interference can be presented in the following form:

$$\mathbf{X}_k = \begin{cases} \xi_k \to \mathcal{H}_0 \ , & k = 1,\ldots,N \\ \mathbf{S}_k + \xi_k \to \mathcal{H}_1 \ , & k = 1,\ldots,N . \end{cases} \tag{21}$$

Covariance matrix of array output under the hypotheses $\mathcal{H}_0$ and $\mathcal{H}_1$ is $\mathbf{R}_0 = \mathbf{R}_\xi$ and $\mathbf{R}_1$ given by (9)–(14), respectively.

Let us assume the interference has characteristics similar to that of the noise and can be absorbed into the noise vector ξ_k. We assume that the noise at the GR PF output can be presented as $\mathbf{R}_\xi = \sigma_\xi^2 \mathbf{I}$, where σ_ξ^2 is the noise variance and the noise power under the hypotheses $\mathcal{H}_0$ and $\mathcal{H}_1$ is not differed. If the noise is spatially coloured or $\mathbf{R}_\xi = \sigma_\xi^2 \mathbf{R}_{\xi\xi}$ where $\mathbf{R}_{\xi\xi}$ is the known positive definite Hermitian matrix, the detection is preceded by the prewhitening filter $\mathbf{R}_{\xi\xi}^{-0.5}$.

We have the binary hypotheses with $\mathbf{X}_k$ being a whitened data vector. We assume that the noise vectors $\{\xi_1,\ldots,\xi_N\}$ are i.i.d. By grouping all the N snapshots of observation vectors into an observation matrix

$$\mathbf{X} = [\mathbf{x}_1,\ldots,\mathbf{x}_N], \tag{22}$$

we have

$$\mathbf{X} = \mathbf{S} + \mathbf{\Xi}, \tag{23}$$

where the signal matrix

$$\mathbf{S} = [\mathbf{s}_1, \ldots, \mathbf{s}_N] \tag{24}$$

and the noise matrix

$$\boldsymbol{\Xi} = [\boldsymbol{\xi}_1, \ldots, \boldsymbol{\xi}_N]. \tag{25}$$

The detection statistics depends on a set of parameters

$$p = \{E_S, \phi, \beta, \sigma_n^2\}. \tag{26}$$

If all parameters are known, this is a standard detection problem whose optimal solution is the GR likelihood ratio [14]–[16]. If the parameters are unknown, we use the GLRT GR involving the replacement of unknown parameters by their maximum likelihood estimates under each hypothesis.

Some specific versions of GR can be constructed depending on what parameters are known or unknown. We consider the GLRT GR in which the conventional beamformers are the counterparts with the same set of unknown parameters so that a fair comparison between the GLRT GR and conventional beamformer can be made.

We consider the following types:

- the GR beamformer type 1 – all the signal parameters are known and this GR is used as a reference;
- the GLRT GR beamformer type 2 – the parameters ϕ, β are unknown;
- the GLRT GR beamformer type 3 – the parameters $E_S, \sigma_n^2, \phi, \beta$ are unknown;
- the GR beamformer type 4 – the parameter ϕ is unknown;
- the GR beamformer type 5 – the parameters ϕ, E_S, σ_n^2 are unknown.

We carry out a comparative analysis between the detectors of types 1, 2, 3, 4, and 5 with the corresponding conventional beamformer. The conventional beamformer is designed assuming the point sources (zero angular spread, i.e. $\beta = 0^\circ$).

4. GR: Specific Modifications

According to the generalized approach to signal processing in noise [14]–[16], the detection problem for the GR can be presented in the following form:

$$\mathbf{X}_k = \begin{cases} \boldsymbol{\xi}_k \to \mathcal{H}_0, & k = 1, \ldots, N \\ \mathbf{S}_k + \boldsymbol{\xi}_k \to \mathcal{H}_1, & k = 1, \ldots, N, \end{cases} \tag{27}$$

where the elements of the vectors ξ_k and η_k, the reference noise at the GR AF output (see Figure 1), are given by (1).

Assume, the target return signals under the hypotheses $\mathcal{H}_0$ and $\mathcal{H}_1$ are the complex Gaussian with zero mean and covariance $\mathbf{R}_0$ and $\mathbf{R}_1$, respectively, and the probability density functions (pdfs) for N observations are given by

$$f(\mathbf{X};\mathcal{H}_0)=[\pi^P \mid \mathbf{R}_0 \mid]^{-N}\exp\{-N\times Tr[\mathbf{R}_0^{-1}\mathbf{Q}']\} \tag{28}$$

and

$$f(\mathbf{X};\mathcal{H}_1)=[\pi^P \mid \mathbf{R}_1 \mid]^{-N}\times\exp\{-N\times Tr[\mathbf{R}_1^{-1}\mathbf{Q}]\}. \tag{29}$$

here,

$$\mathbf{Q}=\frac{1}{N}\sum_{k=1}^{N}[\mathbf{X}_k^{\mathcal{H}_1}][\mathbf{X}_k^{\mathcal{H}_1}]^H=\frac{1}{N}[\mathbf{X}^{\mathcal{H}_1}][\mathbf{X}^{\mathcal{H}_1}]^H \tag{30}$$

and

$$\mathbf{Q}'=\frac{1}{N}\sum_{k=1}^{N}[\mathbf{X}_k^{\mathcal{H}_0}][\mathbf{X}_k^{\mathcal{H}_0}]^H=\frac{1}{N}[\mathbf{X}^{\mathcal{H}_0}][\mathbf{X}^{\mathcal{H}_0}]^H \tag{31}$$

are the sample covariance matrices under the hypotheses $\mathcal{H}_1$ and $\mathcal{H}_0$, respectively. We emphasize that we do not impose the constraint that $N \geq P$, i.e., detection can be carried out based on a single measurement $(N=1)$ or multiple measurements $(N>1)$. Based on the Neyman-Pears-on theorem, when all the parameters are known, the GR test is the logarithm of the likelihood function ratio under the hypotheses $\mathcal{H}_1$ and $\mathcal{H}_0$, i.e.

$$\mathcal{L}(\mathbf{X})=Tr\left\{2\mathbf{S}^H[\mathbf{R}_0^{-1}-\mathbf{R}_1^{-1}]\mathbf{X}^{\mathcal{H}_1}-[\mathbf{X}^{\mathcal{H}_1}][\mathbf{R}_0^{-1}-\mathbf{R}_1^{-1}][\mathbf{X}^{\mathcal{H}_1}]^H+[\mathbf{R}_0^{-1}-\mathbf{R}_1^{-1}]\mathbf{Q}'+N\ln\frac{|\mathbf{R}_0|}{|\mathbf{R}_1|}\right\}. \tag{32}$$

Next, we consider the case when some parameters are unknown. The unknown parameters under the hypotheses $\mathcal{H}_0$ and $\mathcal{H}_1$ are denoted by p_0 and p_1, respectively. In this case, the detection statistic is given by the GLRT [36]

$$l(\mathbf{X},\hat{p}_0,\hat{p}_1)=\frac{\max_{p_1} f(\mathbf{X},\mathcal{H}_1)}{\max_{p_0} f(\mathbf{X},\mathcal{H}_0)} \tag{33}$$

or its logarithm

$$\mathcal{L}(\mathbf{X},\hat{p}_0,\hat{p}_1)=Tr\Big\{2\mathbf{S}^H[\mathbf{R}_0^{-1}(\hat{p}_0)-\mathbf{R}_1^{-1}(\hat{p}_1)]\mathbf{X}^{\mathcal{H}_1}-[\mathbf{X}^{\mathcal{H}_1}][\mathbf{R}_0^{-1}(\hat{p}_0)-\mathbf{R}_1^{-1}(\hat{p}_1)][\mathbf{X}^{\mathcal{H}_1}]^H$$

$$+[\mathbf{R}_0^{-1}(\hat{p}_0)-\mathbf{R}_1^{-1}(\hat{p}_1)]\mathbf{Q}'+N\ln\frac{|\mathbf{R}_0(\hat{p}_0)|}{|\mathbf{R}_1(\hat{p}_1)|}\Big\}, \tag{34}$$

where $\hat{p}_0$ and $\hat{p}_1$ are the parameters maximizing the likelihood function under the hypotheses $\mathcal{H}_0$ and $\mathcal{H}_1$, respectively.

4.1. Subspace GD Beamformer – Known Parameters

Ignoring the constant term $N\ln\frac{|\mathbf{R}_0|}{|\mathbf{R}_1|}$ in (32), we can write

$$\mathcal{L}(\mathbf{X},p)=Tr\Big\{2\mathbf{S}^H\mathbf{B}\mathbf{B}^H\mathbf{X}^{\mathcal{H}_1}-[\mathbf{X}^{\mathcal{H}_1}]\mathbf{B}\mathbf{B}^H[\mathbf{X}^{\mathcal{H}_1}]^H+\mathbf{B}\mathbf{B}^H\mathbf{Q}'\Big\}, \tag{35}$$

where

$$\mathbf{B}\mathbf{B}^H=\mathbf{R}_0^{-1}(p)-\mathbf{R}_1^{-1}(p) \tag{36}$$

and p is defined in (26). The above decomposition of $\mathbf{B}\mathbf{B}^H$ is possible because $\mathbf{R}_0^{-1}-\mathbf{R}_1^{-1}$ is a non-negative definite matrix. In general, $\mathbf{B}$ is the $P\times r$ matrix, $1\le r\le P$. The rank of $\mathbf{B}$ depends on rank of the signal covariance matrix $\mathbf{R}_S$. Utilizing (14) and (19), we obtain

$$\mathbf{R}_1\approx E_S\mathbf{V}_r\mathbf{\Lambda}_r\mathbf{V}_r^H+\mathbf{R}_0. \tag{37}$$

Employing the matrix inversion lemma, we obtain

$$\mathbf{R}_1^{-1}\approx\mathbf{R}_0^{-1}-\mathbf{R}_0^{-1}\mathbf{V}_r[E_S\,\mathbf{\Lambda}_r+\mathbf{V}_r^H\mathbf{R}_0^{-1}\mathbf{V}_r]^{-1}\mathbf{V}_r^H\mathbf{R}_0^{-1}. \tag{38}$$

Hence, we can rewrite (36) as follows:

$$\mathbf{B}\mathbf{B}^H\approx\mathbf{R}_0^{-1}\mathbf{V}_r[E_S\,\mathbf{\Lambda}_r+\mathbf{V}_r^H\mathbf{R}_0^{-1}\mathbf{V}_r]^{-1}\mathbf{V}_r^H\mathbf{R}_0^{-1} \tag{39}$$

and then, the subspace matrix is a $P\times r$ matrix

$$\mathbf{B}=\frac{\mathbf{R}_0^{-1}\mathbf{V}}{\sqrt{E_S\,\mathbf{\Lambda}+\mathbf{V}^H\mathbf{R}_0^{-1}\mathbf{V}}}=[\mathbf{b}_1,\ldots,\mathbf{b}_r]. \tag{40}$$

If the signal subspace is indeed low rank with rank r, the approximation sign is replaced by an equality sign. This leads to an interpretation of the GR as a bank of beamformers. We emphasize, this subspace beamformer is an approximation to the true GR.

In our case, the noise covariance matrix $\mathbf{R}_{\xi} = \sigma_{\xi}^2 \mathbf{I}$ that leads us to a simpler form

$$\mathbf{B} \approx \frac{\mathbf{V}_r}{4\sigma_n^4 \sqrt{\frac{\mathbf{V}_r^H \mathbf{V}_r}{4\sigma_n^4} + E_S \mathbf{\Lambda}}} . \tag{41}$$

We denote $\mathbf{Z}$ as an output matrix of beamformers

$$\mathbf{Z} = \mathbf{B}^H \mathbf{X} = [\mathbf{z}_1, \ldots, \mathbf{z}_N], \tag{42}$$

where $\mathbf{z}_k = \mathbf{B}^H \mathbf{x}_k$ .We will refer to this as a subspace beamformer to distinguish it from the conventional beamformer, where $\mathbf{b}$ is a $P \times 1$ vector. The GR output statistics is given by

$$\mathcal{K}(\mathbf{X}, p) = Tr\{2\mathbf{Z}\mathbf{S}^H - \mathbf{Y}\mathbf{Y}^H + \mathbf{Q}'\} = \sum_{k=1}^{N} \| 2\mathbf{z}_k \mathbf{s}_k^H - \mathbf{z}_k \mathbf{z}_k^H + [\mathbf{x}_k^{\mathcal{H}_0}][\mathbf{x}_k^{\mathcal{H}_0}]^H \|^2 . \tag{43}$$

4.2. GLRT GR – Unknown Parameter $p = \{\phi, \beta, E_S, \sigma_n^2\}$

4.2.1. The Parameter $p = \{\phi, \beta\}$

In this case, the unknown parameter $p = \{\phi, \beta\}$ needs to be estimated. Note that the likelihood function of the GR background noise under the hypothesis $\mathcal{H}_0$ is independent of the signal $\mathbf{S}$ and its parameters p, and thus, it needs to be estimated only under the hypothesis $\mathcal{H}_1$. The detection statistics are constructed as follows by maximizing argument p:

$$\mathcal{K}(\mathbf{X}, \hat{p}_1) = Tr\left\{2\mathbf{S}^H[\mathbf{R}_0^{-1} - \mathbf{R}_1^{-1}(\hat{p}_1)]\mathbf{X}^{\mathcal{H}_1} - [\mathbf{X}^{\mathcal{H}_1}][\mathbf{R}_0^{-1} - \mathbf{R}_1^{-1}(\hat{p}_1)][\mathbf{X}^{\mathcal{H}_1}]^H + [\mathbf{R}_0^{-1} - \mathbf{R}_1^{-1}(\hat{p}_1)]\mathbf{Q}' N \ln \frac{|\mathbf{R}_0(\hat{p}_0)|}{|\mathbf{R}_1(\hat{p}_1)|}\right\}, \tag{44}$$

where

$$\hat{p}_1 = \arg \max_{\phi \in (-0.5\pi, 0.5\pi), \beta \in (0, \beta_0)} \mathcal{K}(\mathbf{X}, p_1) . \tag{45}$$

The estimation is done by a numerical maximization over the range $-\pi \le \phi \le \pi$ or $-0.5\pi \le \phi \le 0.5\pi$ (for a linear array), and $0 \le \beta \le \beta_0$, β_0 is the predetermined angular spread range.

The maximization is carried out by the following steps:

- *Step1*: We divide a two-dimensional search range $\{\phi,\beta\}$ into small grids. The size of the grid $\{\delta\phi,\delta\beta\}$ is a fraction of an array beamwidth. We choose $\delta\beta=\alpha_1 MB$ and $\delta\phi=\alpha_2\times MB$ where $0<\alpha_1,\alpha_2<1$. We find that $\alpha_1,\ \alpha_2=0.5$ produce quite reliable results.
- *Step 2*: For every pair $\{\phi_i,\beta_i\}$, $\mathbf{R}_S(\phi_i,\beta)$ is constructed based on (15).
- *Step 3*: The GR output statistic $\mathcal{K}[\mathbf{X};(\phi_i,\beta_i)]$ is evaluated.
- *Step 4*: This process is repeated, and the largest value of $\mathcal{K}[\mathbf{X};(\phi_i,\beta_i)]$ is selected.

4.2.2. The Parameter $p=\{\phi,\beta,E_S,\sigma_n^2\}$

In this case, all the parameters are unknown. The maximum likelihood estimation procedure requires a nonlinear optimization. The GR searches the global maximum of likelihood function over the unknown parametric sets. The maximization can be carried out as follows:

$$l(\mathbf{X},\hat{E}_S\hat{\sigma}_n^{-2},\hat{\sigma}_S^2,\hat{\sigma}_n^2,\hat{p}_1)=\max_{p_1} l(\mathbf{X},\hat{E}_S\hat{\sigma}_n^{-2},\hat{\sigma}_S^2,\hat{\sigma}_n^2,\hat{p}_1)=\max_{p_1}\max_{\rho\in(0,\rho_0)} l(\mathbf{X},E_S\sigma_n^{-2},\hat{\sigma}_S^2,\hat{\sigma}_n^2,p_1)\,. \tag{46}$$

We first maximize the likelihood function over $(E_S\sigma_n^{-2},\sigma_n^2)$, assuming that $p_1=\{\phi,\beta\}$ is known. We maximize the result over $\{\phi,\beta\}$. The derivation of the maximum likelihood estimators of (E_S,σ_n^2) is provided at the fixed p_1.

The GLRT GR likelihood function takes the following form:

$$l(\mathbf{X},\hat{E}_S\hat{\sigma}_n^{-2},\hat{\sigma}_S^2,\hat{\sigma}_n^2,p_1)=\frac{1}{|\hat{E}_S\hat{\sigma}_n^{-2}\,\mathbf{R}_S(p_1)+\mathbf{I}|^N}\left\{\frac{Tr[\mathbf{Q}]Tr[(\hat{E}_S\hat{\sigma}_n^{-2}\,\mathbf{R}_S(p_1)+\mathbf{I})]}{\mathbf{Q}'}\right\}^{PN}. \tag{47}$$

Taking the logarithm, we obtain the following statistics at the GR output

$$\mathcal{K}(\mathbf{X},\hat{E}_S\hat{\sigma}_n^{-2},\hat{\sigma}_S^2,\hat{\sigma}_n^2,p_1)=PN\ln\left\{\frac{Tr[\mathbf{Q}]Tr[(\hat{E}_S\hat{\sigma}_n^{-2}\,\mathbf{R}_S(\hat{p}_1)+\mathbf{I})]}{\mathbf{Q}'}\right\}-N\ln|\hat{E}_S\hat{\sigma}_n^{-2}\mathbf{R}_S(\hat{p}_1)+\mathbf{I}|\,, \tag{48}$$

$$\hat{p}_1=\arg\max_{-0.5\pi<\phi<0.5\pi,0\le\beta\le\beta_0}\mathcal{K}(\mathbf{X},\hat{E}_S\hat{\sigma}_n^{-2},\hat{\sigma}_S^2,\hat{\sigma}_n^2,p_1)\,. \tag{49}$$

In summary, the maximization is carried out as follows.

- *Step 1*: Follow Steps 1 and 2 in Subsection *4.2.1*.
- *Step 2*: For each pair of $\{\phi_i,\beta_i\}$, a one-dimensional search over ρ is carried out to select the maximal value of $\mathcal{K}(\mathbf{X},\{\phi_i,\beta_i\}E_S\sigma_n^{-2})$. The search can be implemented through a binary search or an exhaustive search and p_0 is a predetermined search range.

- *Step 3*: This process is repeated for all the values of $\{\phi_i, \beta_i\}$ and the largest value of $\mathcal{K}(\mathbf{X}, \{\phi_i, \beta_i\} E_S \sigma_n^{-2})$ is selected.

4.3. GR Beamformer– Unknown Parameter $p = \{\phi, E_S, \sigma_n^2\}$

4.3.1. The Parameter $p = \{\phi\}$

GR beamformer searches for the maximum energy by sweeping over all possible directions. This is the optimal solution (maximum likelihood) for point sources. If the source is distributed, only a fraction of the energy is captured by the beamformer. Degradation in performance will occur.

For a linear array, the beamformer searches over $-0.5\pi \le \phi \le 0.5\pi$. The GR output statistics takes the following form

$$\mathcal{K}(\mathbf{X}) = \| 2\mathbf{S}^H \mathbf{B}\mathbf{B}^H(\hat{\phi})\mathbf{X}^{\mathcal{H}_1} - \mathbf{X}^{\mathcal{H}_1}\mathbf{B}\mathbf{B}^H[\mathbf{X}^{\mathcal{H}_1}]^H + \mathbf{B}\mathbf{B}^H\mathbf{Q}' \|^2 , \tag{50}$$

where

$$\hat{\phi} = \arg \max_{-0.5\pi<\phi<0.5\pi} \| \mathbf{B}^H(\hat{\phi})\mathbf{X} \|^2 \tag{51}$$

and $\mathbf{a}(\phi)$ is the steering vector pointing to direction ϕ. The implementation of this GR beamformer is quite straightforward. The GR beamformer **B** is a normalized steering vector. The maximal value of GR beamformer output statistic is chosen by sweeping the GR beamformer from -0.5π to 0.5π.

4.3.2. The Parameter $p = \{\phi, E_S, \sigma_n^2\}$

The GR beamformer searches the maximum energy output over the range from -0.5π to 0.5π. The signal energy is divided by an estimate of the GR background noise variance that is calculated by projecting GR array output on the subspace orthogonal to the rank 1 steering vector. To exclude the signal power that "leaks" through the beams adjacent to the main beam, we estimate the GR background noise power from beams that are further away from the main beam.

We can choose to exclude the β_0 / MB beams adjacent to the main beam, where β_0 is a predetermined angular spread range. This seemingly *ad hoc* approach is the modified maximum likelihood estimate of the GR background noise variance. It is well known that the GR background noise variance estimate is given by [17], [19]

$$\sigma_g^2 = \| \mathbf{P}_{\mathbf{A}}^{\perp}\mathbf{Q}' \|^2 (P - r_{\mathbf{A}})^{-1} , \tag{52}$$

where $\mathbf{P}_{\mathbf{A}}^{\perp}$ is the projection on the signal subspace **A** and $r_{\mathbf{A}}$ is the signal subspace rank.

The accuracy of the GR background noise estimate will degrade when a smaller subspace is used due to a leakage of the signal power onto the noise subspace. We construct a subspace $\mathbf{C} \subseteq \mathbf{A}$ so that the signal power is excluded from the estimation i.e., the subspace

$$\mathbf{C}(\phi, \beta_0) = \{\mathbf{a}(\phi - 0.5\beta_0), \ldots, \mathbf{a}(\phi + 0.5\beta_0)\} \tag{53}$$

is generated. The power projected onto the null space of $\mathbf{C}(\phi, \beta_0)$ is considered to be the GR background noise power, i.e.

$$\hat{\sigma}_g^2(\phi, \beta_0) = Tr\{\mathbf{P}^{\perp}_{\mathbf{B}(\phi,\beta_0)}\mathbf{Q}'\}(P - r_{\mathbf{B}})^{-1}; \tag{54}$$

$$\mathbf{P}^{\perp}_{\mathbf{B}(\phi,\beta_0)} = \mathbf{I} - \mathbf{P}_{\mathbf{B}(\phi,\beta_0)}; \tag{55}$$

where $r_{\mathbf{C}}$ is the rank of $\mathbf{C}$.

The GR output statistic possessing CFAR properties is given by

$$\mathcal{K}(\mathbf{X}) = \max_{\phi \in (-0.5\pi, 0.5\pi)} \frac{Tr\{2\mathbf{S}^H \mathbf{P}_{\mathbf{a}(\phi)} \mathbf{X}^{\mathcal{H}_1} - \mathbf{X}^{\mathcal{H}_1} \mathbf{P}_{\mathbf{a}(\phi)} (\mathbf{X}^{\mathcal{H}_1})^H + \mathbf{P}_{\mathbf{a}(\phi)}\mathbf{Q}'\}}{\hat{\sigma}_g^2(\phi, \beta_0)}, \tag{56}$$

where $\mathbf{P}_{\mathbf{a}(\phi)}$ is the projection matrix on $\mathbf{a}(\phi)$. The implementation of this GR type involves three steps.

- *Step 1*: For every angle ϕ, we construct a projection matrix $\mathbf{P}_{\mathbf{a}(\phi)}$. The subspace $\mathbf{C}(\phi, \beta_0)$ and null projection matrix $\mathbf{P}_{\mathbf{B}(\phi,\beta_0)}$ are constructed accordingly.
- *Step 2*: The GR output is evaluated based on (54) for every angle ϕ.
- *Step 3*: The largest value of $\mathcal{K}(\mathbf{X}, \{\phi_i, \beta_i\}\rho)$ is selected.

5. Performance Analysis: Known Parameters

5.1. SNR Gain Versus Angular Spread

The *SNR* gain is defined as the ratio of the *SNR* at the radar sensor array GR output to the *SNR* at the radar sensor array GR input. For point sources, *SNR* gain depends on the number of sensors. For a linear array with *P* sensors *SNR* gain is equal to *P*. We derive *SNR* gain for the subspace beamformers. The subspace GR beamformer output takes the following form:

$$\mathbf{z}_k = 2\mathbf{S}^H \mathbf{B}\mathbf{B}^H \mathbf{x}_k^{\mathcal{H}_1} - \mathbf{x}_k^{\mathcal{H}_1} \mathbf{B}\mathbf{B}^H (\mathbf{x}_k^{\mathcal{H}_1})^H + \boldsymbol{\eta}_k \mathbf{B}\mathbf{B}^H \boldsymbol{\eta}_k^H. \tag{57}$$

Let the GR output *SNR* can be presented as the ratio between the average signal and average background noise powers at the beamformer output

$$SNR_{\mathrm{GR}}^{\mathrm{out}} = \frac{Tr\{\mathbf{B}^H E[\mathbf{S}_k \mathbf{S}_k^H]\mathbf{B}\}}{Tr\{\mathbf{B}^H E[\mathbf{Q}']\mathbf{B}\}} = \frac{Tr\{E_S \mathbf{B}^H \mathbf{R}_S \mathbf{B}\}}{Tr\{\mathbf{B}^H \mathbf{R}_\xi \mathbf{R}_\xi^H \mathbf{B}\}} = \frac{E_S}{\sigma_\xi^2} \times \frac{Tr\{E_S \mathbf{B}^H \mathbf{R}_S \mathbf{B}\}}{Tr\{\mathbf{B}^H \mathbf{R}_\xi \mathbf{R}_\xi^H \mathbf{B}\}} . \tag{58}$$

The GR input *SNR* is defined as E_S / σ_n^2. The *SNR* gain is given by

$$\frac{SNR_{\mathrm{GR}}^{\mathrm{out}}}{SNR_{GR}^{in}} = \frac{Tr\{E_S \mathbf{B}^H \mathbf{R}_S \mathbf{B}\}}{Tr\{\mathbf{B}^H \mathbf{B}\}} . \tag{59}$$

We are interested in how the *SNR* gain of the subspace GR beamformer is varied with the signal angular spread. Note that

$$\mathbf{B}\mathbf{B}^H = 0.25\sigma_\xi^{-4}\mathbf{I} - [4\sigma_\xi^4 \mathbf{I} + E_S \mathbf{R}_S(\beta)]^{-1} \approx \mathbf{V}_r \{0.25\sigma_\xi^{-4}\mathbf{I} - [4\sigma_\xi^4 \mathbf{I} + E_S \mathbf{\Lambda}_r]^{-1}\}\mathbf{V}_r^H = \mathbf{V}_r \mathbf{D} \mathbf{V}_r^H , \tag{60}$$

where

$$\mathbf{D} = 0.25\sigma_n^{-4}\mathbf{I} - [4\sigma_n^4 \mathbf{I} + E_S \mathbf{\Lambda}_r]^{-1} . \tag{61}$$

Then, the *SNR* gain is defined as

$$\frac{SNR_{\mathrm{GR}}^{\mathrm{out}}}{SNR_{GR}^{in}} = \frac{Tr\{\mathbf{D}\,\mathbf{\Lambda}_r\}}{Tr\{\mathbf{D}\}} = \frac{\sum_{i=1}^{r} \lambda_i^2 [1 + SNR \times \lambda_i]^{-1}}{\sum_{i=1}^{r} \lambda_i [1 + SNR \times \lambda_i]^{-1}} . \tag{62}$$

For simplicity, we assume that the dominant eigenvalues are approximately equal, i.e., $\lambda_i = P/r$, $i = 1,\ldots,r$. This approximation is certainly not very accurate, but it reveals some insights of the *SNR* gain behaviour. Therefore, we obtain

$$\frac{SNR_{\mathrm{GR}}^{\mathrm{out}}}{SNR_{GR}^{in}} \approx \frac{P}{r} . \tag{63}$$

This result shows that the *SNR* gain for the subspace GR beamformer not only depends on the number of sensors P but on the source angular spread β through the subspace rank r as well. It is a monotone decreasing function of r. The following can be concluded as two special cases:

- In the point source case $\beta = 0^\circ$ or $\mathbf{R}_S = \mathbf{a}\mathbf{a}^H$, we get the *SNR* gain equal to P;
- In the case $\beta = 180^\circ$ or $\mathbf{R}_S = \mathbf{I}$, we get the unit *SNR* gain.

5.2. Receiver Operating Characteristics (ROC)

We derive the analytical expression for pdfs under two hypotheses $\mathcal{H}_0$ and $\mathcal{H}_1$. By $\chi^2_M(z)$ and $f_M(z)$ we denote the central Chi-squared distribution with M degrees of freedom and the pdf of the central Chi-squared distribution with M degrees of freedom, respectively. Log-likelihood ratios at the hypotheses $\mathcal{H}_0$ and $\mathcal{H}_1$ can be represented by sum of quadratic forms in complex Gaussian random variables

$$\mathcal{L}(\mathbf{X},\mathcal{H}_0)=\mathbf{B}\mathbf{B}^H\mathbf{Q}'-\mathbf{X}^H_{\mathcal{H}_0}\mathbf{B}\mathbf{B}^H\mathbf{X}_{\mathcal{H}_0}=\sum_{k=1}^{N}\boldsymbol{\eta}_k^H\mathbf{R}_0^{-1}\boldsymbol{\eta}_k-\sum_{k=1}^{N}\boldsymbol{\xi}_k^H\mathbf{R}_0^{-1}\boldsymbol{\xi}_k$$

$$=\sum_{k=1}^{N}\left[\sum_{j=1}^{r}\lambda_j\,|\,\mathbf{v}_j^H\boldsymbol{\eta}_k\,|^2-\sum_{j=1}^{r}\lambda_j\,|\,\mathbf{v}_j^H\boldsymbol{\xi}_k\,|^2\right]; \tag{64}$$

$$\mathcal{L}(\mathbf{X},\mathcal{H}_1)=2\mathbf{S}^H\mathbf{R}_S\mathbf{X}_{\mathcal{H}_1}+\mathbf{B}\mathbf{B}^H\mathbf{Q}'-\mathbf{X}^H_{\mathcal{H}_1}\mathbf{B}\mathbf{B}^H\mathbf{X}_{\mathcal{H}_1}$$

$$=\sum_{k=1}^{N}\mathbf{S}_k^H(\mathbf{R}_0^{-1}-\mathbf{R}_1^{-1})\mathbf{S}_k+\sum_{k=1}^{N}\boldsymbol{\eta}_k^H\mathbf{R}_0^{-1}\boldsymbol{\eta}_k-\sum_{k=1}^{N}\boldsymbol{\xi}_k^H\mathbf{R}_0^{-1}\boldsymbol{\xi}_k$$

$$=\sum_{k=1}^{N}\left[\sum_{j=1}^{r}\lambda_j\,|\,\mathbf{v}_j^H\mathbf{S}_k\,|^2+\sum_{j=1}^{r}\lambda_j\,|\,\mathbf{v}_j^H\boldsymbol{\eta}_k\,|^2-\sum_{j=1}^{r}\lambda_j\,|\,\mathbf{v}_j^H\boldsymbol{\xi}_k\,|^2\right]; \tag{65}$$

where λ_j are nonzero eigenvalues of the matrix $\mathbf{B}\mathbf{B}^H$ and $\mathbf{v}_j$ are the associated eigenvectors.

Thus, we can write

$$\mathcal{L}(\mathbf{X},\mathcal{H}_i)=\sum_{k=1}^{N}\sum_{j=1}^{r}\gamma_{ji}\,|\,z_{jik}\,|^2,\qquad i=0,1 \tag{66}$$

where z_{jik} are independent zero mean and unit variance complex Gaussian random variables and $\{\gamma_{ji}, j=1,\ldots,r\}$ are the r real nonzero weights. More precisely,

$$\begin{cases}\gamma_{j0}=E_S\lambda_j(E_S\lambda_j+4\sigma_\xi^4)^{-1},\\ \gamma_{j1}=0.25E_S\lambda_j\sigma_\xi^{-4},\\ \quad j=1,\ldots,r\end{cases} \tag{67}$$

where λ_j are the eigenvalues of $\mathbf{R}_S$.

As an extension of the results in [37] and [38] from real to complex numbers, the quadratic form $\mathcal{L}(\mathbf{X},\mathcal{H}_i)$ is distributed approximately as the scaled Chi-squared random variable, or $\mathcal{L}(\mathbf{X},\mathcal{H}_i)\sim\delta_i\chi^2_{M_i}$, where the scaling factor δ_i and the degrees of freedom M_i are given by

$$\delta_i = \frac{\sum_{i=0}^{1}\sum_{j=1}^{r}\gamma_{ij}^2}{\sum_{i=0}^{1}\sum_{j=1}^{r}\gamma_{ij}}, \quad M_i = 2N\frac{\left[\sum_{i=0}^{1}\sum_{j=1}^{r}\gamma_{ij}\right]^2}{\sum_{i=0}^{1}\sum_{j=1}^{r}\gamma_{ij}^2}. \tag{68}$$

Plugging (67) into (68), we obtain

$$\delta_0 = \frac{\sum_{j=1}^{r}\left[\frac{SNR^{in}\lambda_j}{SNR^{in}\lambda_j+4\sigma_n^2}\right]^2}{\sum_{j=1}^{r}\frac{SNR^{in}\lambda_j}{SNR^{in}\lambda_j+4\sigma_n^2}}, M_0 = 2N\frac{\left\{\sum_{j=1}^{r}\frac{SNR^{in}\lambda_j}{SNR^{in}\lambda_j+4\sigma_n^2}\right\}^2}{\sum_{j=1}^{r}\left[\frac{SNR^{in}\lambda_j}{SNR^{in}\lambda_j+4\sigma_n^2}\right]^2}; \tag{69}$$

$$\delta_1 = \frac{SNR^{in}}{4\sigma_n^2 P}\sum_{j=1}^{r}\lambda_j^2, M_1 = \frac{2NP^2}{\sum_{j=1}^{r}\lambda_j^2}. \tag{70}$$

Utilizing the Jacobean transformation, we can show that the pdf of detection statistics $\mathscr{L}(\mathbf{X},\mathscr{H}_i)$ is defined by $|\delta_i|^{-1} f_{M_i}(z_i\delta_i^{-1})$. Note that the absolute sign can be ignored because δ_i is a positive number. This leads to an approximation of the probability of false alarm

$$P_{AF} \approx \int_{K_g}^{\infty} f_{M_0}(z)dz \tag{71}$$

and the probability of detection

$$P_D \approx \int_{(\delta_0/\delta_1)K_g}^{\infty} f_{M_1}(z)dz, \tag{72}$$

where the pdf is given by

$$f_{M_i}(u) = 0.5^{0.5M_i}[\Gamma(0.5M_i)]^{-1}u^{0.5M_i-1}\exp\{-0.5u\}. \tag{73}$$

Let

$$F_M(u) = \int_0^u f_M(z)dz \tag{74}$$

is the probability distribution function of Chi-squared random variable with M degrees of freedom and $F_M^{-1}(u)$ is the inverse probability distribution function.

The probability of false alarm P_{AF} and the probability of detection P_D of quadratic form $\mathcal{K}(\mathbf{X},\mathcal{H}_i)$ can be written as

$$\begin{cases} P_{FA} \approx 1 - F_{M_0}(u); \\ P_D \approx 1 - F_{M_1}(\delta_0 u/\delta_1). \end{cases} \tag{75}$$

For a fixed level of false alarm rate, we have a closed-form expression of the probability of detection

$$P_D \approx 1 - F_{M_1}\left[\delta_0 F_{M_0}^{-1}(1 - P_{FA})/\delta_1\right]. \tag{76}$$

Computer simulation demonstrates that the analytical result (the lines) is matched with the Monte Carlo simulation result (the markers) quite well for different number of measurements, signal angular spreads, and false alarm rates. The asymptotic performance of the probability of detection P_D as N is sufficiently large can also be obtained based on the fact that the Chi-squared pdf with M degrees of freedom tends to approach a Gaussian normal pdf with mean M and variance $2M$. If M is sufficiently great in magnitude

$$F_M(u) \to \Psi\left[u - M(2M)^{-0.5}\right], \tag{77}$$

where

$$\Psi(u) = \int_{-\infty}^{u} (2\pi)^{-0.5} \exp\{-0.5u^2\} du. \tag{78}$$

We obtain

$$P_D \approx 1 - \Psi\left\{\frac{\frac{\delta_0}{\delta_1}\left[M_0 + \sqrt{2M_0}\Psi^{-1}(1 - P_{FA})\right] - M_1}{\sqrt{2M_1}}\right\}. \tag{79}$$

5.3. Required *SNR* (*RSNR*)

The ROC describes behaviour of the probability of detection P_D as a function of the *SNR* that changes the given probability of false alarm P_{FA}. To compare different GR performance it is sometimes convenient to define a scalar performance measure, rather than to use the entire ROC curve.

We define the *RSNR* as the *SNR* needed to produce the probability of target detection at a given false alarm rate. Another quantity of interest is the GR output *SNR* required to achieve the same target probability of detection P_D for the fixed probability of false alarm P_{FA}. From (69) and (70) we obtain

$$\frac{\delta_1}{\delta_0} = \frac{F_{M_1}^{-1}(1-P_{FA})}{F_{M_0}^{-1}(1-P_D)}. \tag{80}$$

Simplification leads us to

$$RSNR = \frac{P}{\sum_{j=1}^{r}\lambda_j^2} \times \frac{\left\{\sum_{j=1}^{r}\frac{SNR^{in}\lambda_j}{SNR^{in}\lambda_j+4\sigma_n^2}\right\}^2}{\sum_{j=1}^{r}\left[\frac{SNR^{in}\lambda_j}{SNR^{in}\lambda_j+4\sigma_n^2}\right]^2} \times \frac{F_{M_1}^{-1}(1-P_{FA})}{F_{M_0}^{-1}(1-P_D)}. \tag{81}$$

The general behaviour of the quantity *RSNR* depends on eigenvalues, which has certain distributions [38]. Equation (77) is quite complicated. To gain some insights of this quantity, we look at the case where all the principal eigenvalues of $\mathbf{R}_S$ are approximately equal, i.e., $\lambda_i = \lambda = P/r, i = 1,\ldots,r$. This approximation is certainly not accurate but serves for simplicity purposes to illustrate the performance of *RSNR* as the degrees of freedom changes. A more accurate result may be obtained by a numerical approach. With this assumption, we have $M_0 \approx 2Nr, M_1 \approx 2Nr$. Let $v = 2Nr$ denotes the degrees of freedom, and after some transformations, we obtain

$$RSNR = \frac{v}{2P} \times \frac{F_v^{-1}(1-P_{FA})}{F_v^{-1}(1-P_D)-1} \tag{82}$$

and the quantity *RSNR* is given as

$$RSNR = \frac{SNR_{\mathrm{GR}}^{\mathrm{out}}}{SNR_{\mathrm{GR}}^{\mathrm{in}}} \approx N \times \frac{F_v^{-1}(1-P_{FA})}{F_v^{-1}(1-P_D)-1}. \tag{83}$$

The quantity *RSNR* that is a function of (v, P_D, P_{FA}) can be easily evaluated by numerical method. For the fixed probability of false alarm P_{FA}, Figure 2 depicts the *RSNR* for different values of degrees of freedom v and the probability of detection P_D.

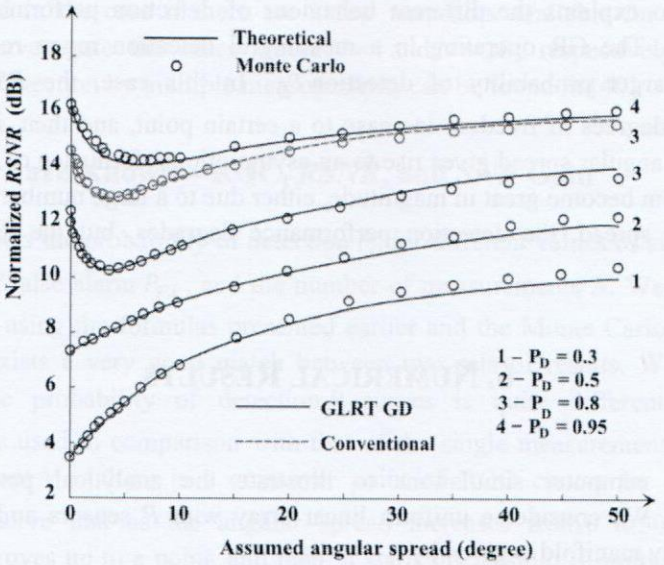

Figure 2. Normalized *RSNR* versus degrees of freedom $v \in [1,50]$ at various P_D ; $P_{FA} = 10^{-3}$.

To eliminate the effect of size of the linear array, we multiply the *RSNR* by array size *P*. It is easy to see that the normalized *RSNR*, e.g. $P \times RSNR$ is a quantity that depends on the degrees of freedom *v*, the probability of detection P_D , and the probability of false alarm P_{FA} . This observation indicates that although the increase of the angular spread causes a reduction of the *SNR* gain, it changes the distribution of the detection statistics by increasing its degrees of freedom.

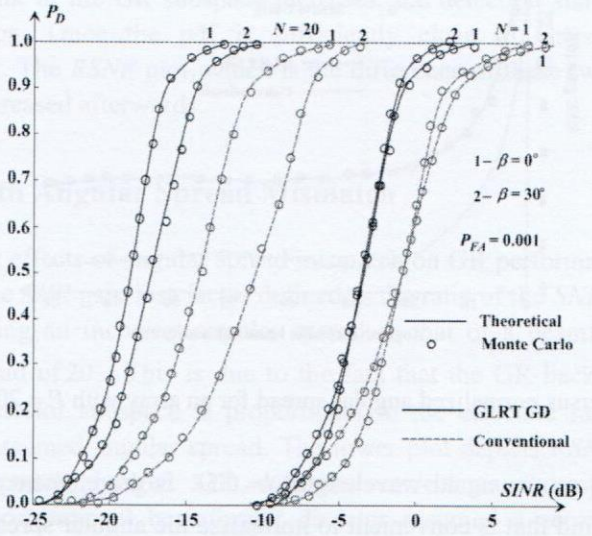

Figure 3. P_D versus *SNR*; all parameters are known; the number of sensors $P = 20$.

Figure 2 also explains the different behaviour of detection performance presented in Figures 3 and 4. The GR operating in a meaningful detection range requires a great in magnitude the target probability of detection P_D. In this case, the *RSNR* performance improves as the degrees of freedom increase to a certain point, and then, it starts dropping. Large N or large angular spread gives rise to an asymptotic performance of the *RSNR*. As the degrees of freedom become great in magnitude, either due to a large number of measurements or large angular spread, the detection performance degrades, but the degradation is not significant.

6. NUMERICAL RESULTS

We present computer simulations to illustrate the analytical performance results discussed above. We consider a uniform linear array with P sensors and half wavelength spacing. The array manifold is given by

$$\mathbf{a}(\phi) = \left[1, e^{j\frac{2\pi}{\lambda}d\sin\phi}, \ldots, e^{j\frac{2\pi(P-1)}{\lambda}d\sin\phi}\right]^T, \tag{84}$$

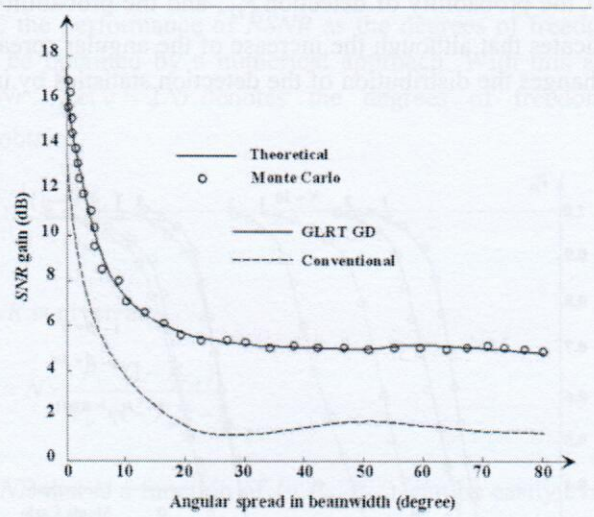

Figure 4. *SNR* gain versus normalized angular spread for an array with $P = 20$ sensors.

where λ is the target return signal wavelength, $d = 0.5\lambda$ is the element spacing, and ϕ is the azimuth angle. We find that is convenient to normalize the angular spread by the array beam width [39]. We assign $P = 20$. Thus, the beam width of this linear array is equal to 6.03°. We assume that the source is located at 20° relative to the broadside of the array. Throughout the simulation, the probability of false alarm $P_{FA} = 10^{-3}$ and the probability of detection $P_D = 0.8$.

We are interested in the case if there are a few snapshots available for detection. In the simulation, we investigate the cases where $N = 1$ and $N = 20$, respectively. More detailed discussion about detection by multiple measurements can be found in [40].

6.1. Parameters are Known – ROC, *RSNR*, and *SNR* Gain

Figure 3 depicts the probability of detection P_D for different values of angular spreads β, the probability of false alarm P_{FA}, and the number of measurements N. We can see both the analytical results using the formulas presented earlier and the Monte Carlo trial results. We note that there exists a very good match between two sets of results. We notice that the behaviour of the probability of detection P_D curves is quite different when multiple measurements are used in comparison with that of the single measurement detection. For a single measurement $N = 1$ there is a crossover point of ROC curves for different angular spreads. We observe that as the angular spread increases from 0° to 30°, the detection performance improves up to a point, and then, it starts decreasing. If multiple measurements are used, the detection performance drops as the angular spread increases. This phenomenon is due to the change of the pdf shape, whose degrees of freedom are affected by both the angular spread and the number of measurements. Alternative way to look this phenomenon is to investigate the *RSNR* as a function of the angular spread. Figure 3 demonstrates a superiority of GLRT GR employment in comparison with the conventional beamformer.

Figure 4 shows the behaviour of the *SNR* gain as a function of the angular spread. The *SNR* gain plot decreases monotonically from 17 to 5 dB as the angular spread increases from $\beta = 0^\circ$ to $\beta = 360^\circ$. The GR output *RSNR* demonstrates a performance improvement caused by the GR output statistics pdf change as the angular spread increases. As the angular spread and the effective rank of the GR subspace increases, the detection statistics pdf becomes a Gaussian distribution. Once the pdf is sufficiently close to Gaussian one, no more improvement occurs. The *RSNR* plot, which is the difference of these two plots, is decreased up to a point and increased afterwards.

6.2. Detection with Angular Spread Mismatch

We examine the effects of angular spread mismatch on GR performance. In Figure 5, the upper plot depicts the *SNR* gain loss factor defined as the ratio of the *SNR* gain for a subspace GR beamformer using an incorrect angular spread to that of a beamformer that uses the correct angular spread of 20°. This is due to the fact that the GR background noise power projected on the detector subspace is proportional to the effective rank of subspace that increases with the assumed angular spread. The lower plot depicts *RSNR* loss factor as the assumed angular spread changes. GR with the correct angular spread has the best performance. The conventional beamformer detector assumed a zero angular spread and experienced a loss of approximately 7 dB in this case.

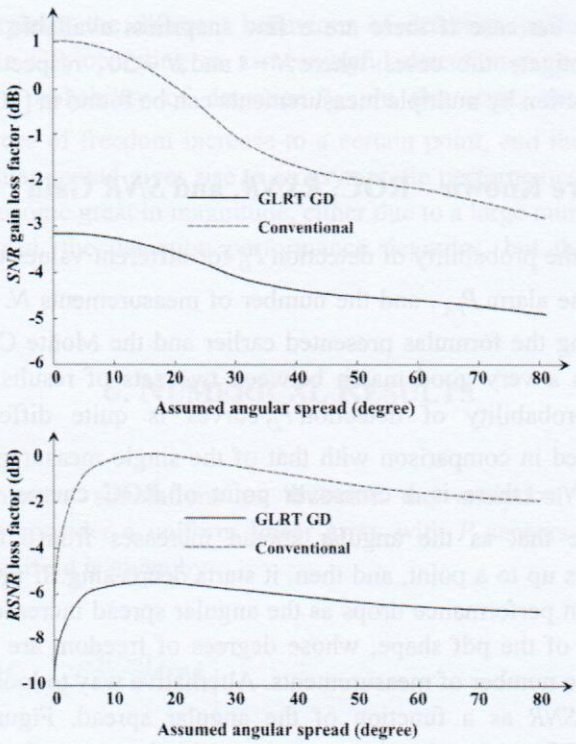

Figure 5. *RSNR* and *SNR* gain loss factor versus assumed angular spread when there is an angular mismatch; the number of sensors $P = 20$; the angular spread $\beta = 20^{\circ}$.

6.3. Detection Performance as a Function of Angular Spread

At the fixed probability of false alarm $P_{FA} = 10^{-3}$ we study the probability of detection P_D. GLRT GR detector searches over ranges of direction ϕ and angular spread β the maximal value of likelihood function. Searching is carried out over the range $-90^{\circ} \le \phi \le 90^{\circ}$ and $0 \le \beta \le \beta_0$, where β_0 is set to be 60°.

Figures 6 and 7 depict the probability of detection P_D and *RSNR* versus angular spread for different detectors with single measurement, i.e., $N = 1$. The results show that when the angular spread is small there is a little difference between the GLRT GR and GR beamformer because the source is appeared to be a point-like source. The main beam of the GR beamformer is able to capture all the energy coming from the source. Actually, the GLRT GR has slightly worse performance than that of the GR beamformer due to the excessive search which results in an increase of detection threshold. As the angular spread gets larger, the performance of both GLRT GR and GR beamformer degrades. The degradation of GR beamformer is much more significant than that of GLRT GR. In the case of large angular spread the GLRT GR demonstrates the better probability of detection P_D in comparison with the GR beamformer.

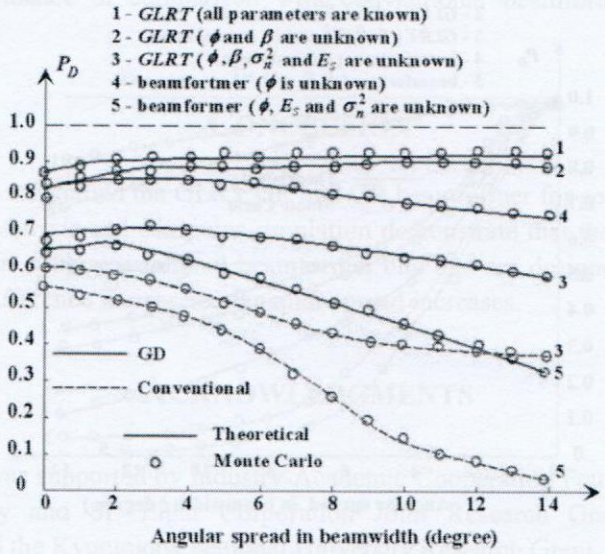

Figure 6. P_D versus normalized angular spread; the number of measurement is $N = 1, SNR = 2\text{dB}$, $P_{FA} = 10^{-3}$.

We plot the results in the case of known parameters to see how much the detection performance degrades than occurs for other suboptimal detectors. We study the GR performance when multiple measurements $N = 20$ are used. We compare the probability of detection P_D and *RSNR* when the parameters are unknown (see subsections 4.2 and 4.3) at $N = 20$ data snap-shots.

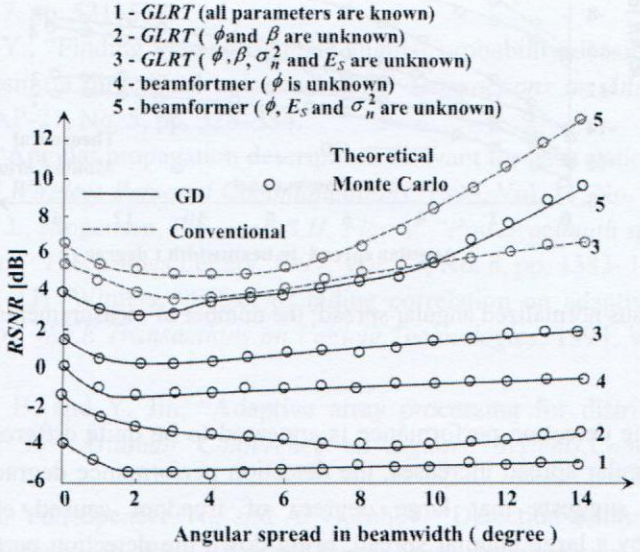

Figure 7. *RSNR* versus normalized angular spread; the number of measurement is $N = 1, P_D = 0.8$, $P_{FA} = 10^{-3}$.

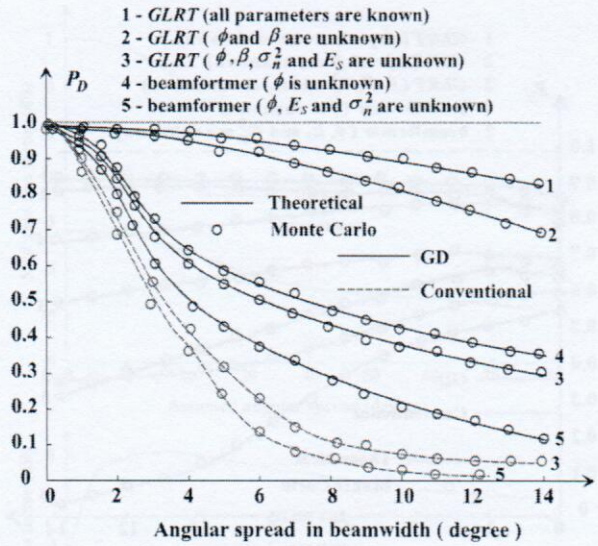

Figure 8. P_D versus normalized angular spread; the number of measurements is $N = 20, SNR = -8\text{dB}, P_{FA} = 10^{-3}$.

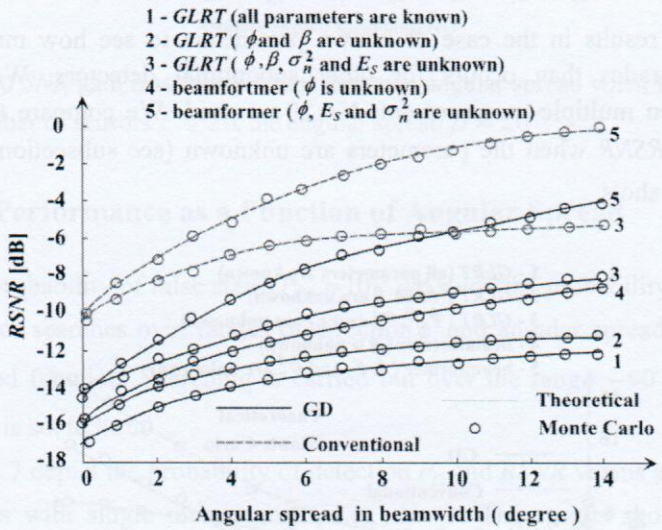

Figure 9. *RSNR* versus normalized angular spread; the number of measurements is $N = 20, P_D = 0.8, P_{FA} = 10^{-3}$.

We see that the detection performance is appeared to be quite different than at $N = 1$. If $N = 20$, as the angular spread increases, the detection performance degrades monotonically. This observation suggests that large degrees of freedom caused either by multiple measurements or by a large angular spread, bring down the detection performance. The GR beamformer detection performance degrades faster in comparison with GLRT GR one. Simulation results in Figures 8 and 9 also demonstrate the better GLRT GR and GR

beamformer performance in comparison with conventional beamformers as the angular spread increases.

CONCLUSION

In this chapter, we studied the GLRT GR and GR beamformer for spatially distributed signal sources. The analysis and computer simulation demonstrate that the GR performance is better in comparison with conventional beamformer one that are designed for point sources. The performance difference increases as angular spread increases.

ACKNOWLEDGMENTS

This research was supported by Industry-Academic Cooperation Foundation, Kyungpook National University and SL Light Corporation Joint Research Grant (the Grant No. 201014590000) and the Kyungpook National University Research Grant, 2013.

REFERENCES

[1] Adachi, F., Freeney, M.T., Williamson, A.G., and D. Parson, "Cross correlation between the envelopes of 900 MHz signals received at a mobile radio base station site," in *Proceedings of Institute of Electrical Engineers F*, 1991, Vol. 133, No. 6, pp. 506–512.

[2] Ikegami, F. and S. Yoshida, "Analysis of multipath propagation structure in urban mobile radio environments," *IEEE Transactions on Antenna Propagation*, 1980, Vol. AP-28, No. 7, pp. 531–537.

[3] Lee, W. C.-Y., "Finding the approximate angular probability density function of wave arrival by using a directional antenna," *IEEE Transactions on Antenna Propagation*, 1973, Vol. AP-21, No. 5, pp. 328–334.

[4] Eggers, P., "Angular propagation descriptions relevant for base station adaptive antenna operations," *Wireless Personal Communications*, 1999, Vol. 11, No. 10, pp. 3–29.

[5] Pedersen, K.I., Mogensen, P.E., a*nd B.H. Fleury, "Power azimuth spectrum in outdoor environments,"* Electronics Letters, 1997, Vol. 33, No. 8, pp. 1583–1584.

[6] Salz, J. and J.H. Winters, "Effect of fading correlation on adaptive arrays in digital mobile radio," *IEEE Transactions on Vehicle Technologies*, 1994, Vol. 43, No. 11, pp. 1049–1057.

[7] Friedlander, B. and Y. Jin, "Adaptive array processing for distributed sources," in *Proceedings 35th Asilomar Conference on Signals, Systems,Computers*, November 2001.

[8] Abramovich, Yu., Spencer, N., and A. Gorohov, "Detection-estimation of distributed Gaussian sources," in *Proceedings Sensor Array Multichannel Signal Processing Workshop*, 2002, pp. 513–517.

[9] Besson, O. and P. Stoica, "Decoupled estimation of DOA and angular spread for a spatially distributed source," *IEEE Transactions on Signal Processing*, 2000, Vol. 48, No. 7, pp.1872–1882.

[10] Raich, R., Goldberg, J., and H. Messer, "Bearing estimation for a distributed source: Modelling, inherent accuracy limitations and algorithm," *IEEE Transactions on Signal Processing*, 2000, Vol. 48, No. 2, pp.429–441.

[11] Valaee, S., Champagne, B., and P. Kabal,"Parametric localization of distributed sources," *IEEE Transactions on Signal Processing*, 1995, Vol. 43, No. 9, pp. 2144–2153.

[12] Raghavan, R.S., Pulsone, N., and D.J. McLauhlin, "Performance of the GLRT for adaptive vector subspace detection," *IEEE Transactions on Aerospace Electronics Systems*, 1996, Vol. 32, No. 10, pp.1473–1487.

[13] Scharf, L.L. and B. Friedlander, "Matched subspace detection," *IEEE Transactions on Signal Processing*, 1994, Vol. 42, No. 8, pp. 2146–2157.

[14] Tuzlukov, V.P., "A new approach to signal detection theory," *Digital Signal Processing*, 1998, Vol. 8, No. 3, pp. 166–184.

[15] Tuzlukov, V.P., *Signal Processing in Noise: A New Methodology*. Minsk: IEC, 1998.

[16] Tuzlukov, V.P., *Signal Detection Theory*. New York: Springer-Verlag, 2001

[17] Tuzlukov, V.P., *Signal Processing Noise*. Boca Raton, London, New York, Washington D.C.: CRC Press, Taylor & Francis Group, 2002.

[18] Tuzlukov, V.P., *Signal and Image Processing in Navigational Systems*. Boca Raton, London, New York, Washington D.C.: CRC Press, Taylor & Francis Group, 2005.

[19] Tuzlukov, V.P., *Signal Processing in Radar Systems*. Boca Raton, London, New York, Washington D.C. CRC Press, Taylor & Francis Group, 2012.

[20] Tuzlukov, V.P.,"DS-CDMA downlink systems with fading channel employing the generalized receiver," *Digital Signal Processing*, 2011, Vol. 21, No. 6, pp. 725–733.

[21] [21] Tuzlukov, V.P., "Signal processing by generalized receiver in DS-CDMA wireless communication systems with frequency-selective channels," *Circuits, Systems, and Signal Processing*, 2011,Vol. 30, No. 6, pp.1197–1230.

[22] Tuzlukov, V.P., "Signal processing by generalized receiver in DS-CDMA wireless communication systems with optimal combining and partial cancellation," *EURASIP Journal on Advances in Signal Processing*, Vol. 2011, Article ID 913189, 15 pages, 2011, doi:10.1155/2011/913189.

[23] Tuzlukov, V.P. "Generalized approach to signal processing in wireless communications: the main aspects and some examples," Ch. 11 in *Wireless Communications and Networks: Recent Advances*. Editor: Eksim Ali, InTech, Croatia, 2012, pp. 305–338.

[24] Tuzlukov, V.P., "Wireless communications: generalized approach to signal processing," Ch. 6 in *Communication Systems: New Research*. Editor: Vyacheslav Tuzlukov, NOVA Science Publisher, Inc., New York, USA, 2013, pp. 175–268.

[25] Tuzlukov, V.P., "Signal processing by generalized receiver in DS-CDMA wireless communication Systems," Ch. 4 in *Countemporary Issues in Wireless Communications*. Editor: Mutamed Khatib, InTech, Croatia, 2014, pp. 79–158.

[26] Shbat, M.S. and V.P. Tuzlukov, "Radar sensor detectors for vehicle safety systems," Ch. 1 in *Autonomous Hybrid Vehicles: Intelligent Transport Systems and Automotive*

Technologies. Editors: Nicu Bizon, Lucian Dascalescu, and Naser Tabatabaei, Publishing House, University of Pitesti, Romania, 2013, pp. 1–27.

[27] Shbat, M.S. and V.P. Tuzlukov, "Radar sensor detectors for vehicle safety systems," Ch.1 in *Autonomous Vehicles: Intelligent Transport Systems and Smart Technologies*. Editors: Nicu Bizon, Lucian Dascalescu, and Naser Tabatabaei, Nova Science Publishers, Inc., New York, 2014, pp. 3–56.

[28] Shbat, M.S. and V.P. Tuzlukov,"Evaluation of detection performance under employment of generalized detector in radar sensor systems," *Radioengineering*, 2014, Vol. 23, No. 1, pp. 50–65.

[29] Shbat, M.S. and V.P. Tuzlukov, "Generalized detector with adaptive detection threshold for radar sensors," in Proc. *International Radar Symposium (IRS 2012)*, Warsaw, Poland, 2012, pp. 91–94.

[30] Shbat, M.S. and V.P. Tuzlukov, "Noise power estimation under generalized detector employment in automotive detection and tracking systems," in *Proc. 9th IET Data Fusion and Target Tracking Conf. (DF&TT'12)*, London, UK, 2012, doi: 10.1049/cp. 2012.0416.

[31] Shbat, M.S. and V.P. Tuzlukov, "Definition of adaptive detection threshold under employment of the generalized detector in radar sensor systems," *IET Signal Processing*, 2014, Vol. 8, Issue 6, pp. 622–632.

[32] Shbat, M.S. and V.P. Tuzlukov, "Spectrum sensing under correlated antenna array using generalized detector in cognitive radio systems," *International Journal of Antennas and Propagation*, vol. 2013, Article ID 853746, 8 pages, 2013, doi:10.1155/2013/ 853746.

[33] Maximov, M., "Joint correlation of fluctuative noise at outputs of frequency filters," *Radio Engineering,* No. 9, 1956, pp.28–38.

[34] Chernyak, Yu. "Joint correlation of noise voltage at outputs of amplifiers with nonoverlapping responses," *Radio Physics and Electronics*, No. 4, 1960, pp. 551–561.

[35] Shbat, M.S. "Performance analysis of signal detection by GD in radar sensor and cognitive radio systems," Kyungpook National University, PhD Thesis, 131 p., December 2013.

[36] Lehmann, E., Testing Statistical Hypotheses, 2nd Ed. New York: Wiley-Interscience, 1986.

[37] Box, G.E.P., "Some theorems on quadratic forms applied in the study of analysis of variance problems, I. Effect of inequality of variance in the one-way classification," *Annual Mathematical Statistics*, 1954, Vol.25, No. 2, pp. 290–302.

[38] Lee, H.B., "Eigenvalues and eigenvectors of covariance matrices for signals closely spaced in frequency," *IEEE Transactions on Signal Processing*, 1992, Vol. SP-40, No. 10, pp. 2518–2535.

[39] Ma, M.T., Theory and Application of Antenna Array, New York: Wiley, 1974.

[40] Helstrom, C.W., Statistical Theory of Signal Detection, 2nd Ed. New York: Pergamon, 1968.